At-wavelength testing of optics for EUV

Kenneth A. Goldberg, H. Raul Beguiristain, Jeffrey Bokor, Hector Medecki, Keith H. Jackson, et al.

Kenneth A. Goldberg, H. Raul Beguiristain, Jeffrey Bokor, Hector Medecki, Keith H. Jackson, David T. Attwood, Gary E. Sommargren, James P. Spallas, Ralph E. Hostetler, "At-wavelength testing of optics for EUV," Proc. SPIE 2437, Electron-Beam, X-Ray, EUV, and Ion-Beam Submicrometer Lithographies for Manufacturing V, (19 May 1995); doi: 10.1117/12.209172

SPIE.

Event: SPIE's 1995 Symposium on Microlithography, 1995, Santa Clara, CA, United States

At-wavelength testing of optics for EUV

K. A. Goldberg[a,b], R. Beguiristain[a,c], J. Bokor[a,d], H. Medecki[a], K. Jackson[a], D. T. Attwood[a,d], G. E. Sommargren[e], J. P. Spallas[e], R. Hostetler[f]

[a]Center for X-Ray Optics, Lawrence Berkeley Laboratory, Berkeley, CA 94720
[b]Department of Physics, University of California, Berkeley 94720
[c]Department of Nuclear Engineering, University of California, Berkeley 94720
[d]Department of Electrical Engineering and Computer Science, University of California, Berkeley 94720
[e]Advanced Microtechnology Program, Lawrence Livermore National Laboratory, Livermore, CA 94550
[f]Ray Raskin Associates, Livermore, CA 94550

ABSTRACT

Optical systems for extreme ultraviolet (EUV) lithography require optical elements with wavefront aberrations limited to a fraction of an EUV wavelength to achieve diffraction-limited performance. Achieving wavefront and surface figure metrology at this level of accuracy is one of the key challenges in the development of EUV lithography. We have successfully built and operated a prototype EUV point diffraction interferometer which is capable of performing wavefront measurement of EUV optical elements at their operational wavelength. Initial experiments to characterize the interferometer, and to measure the optical wavefront diffracted from a Fresnel zone plate lens are discussed.

Keywords: extreme ultraviolet lithography, interferometry, point diffraction interferometer, Fresnel zone plate lens, EUV

2. INTRODUCTION

Optical elements for extreme ultraviolet (EUV) lithography have surface figure error tolerances in the sub-nanometer regime.[1] These stringent requirements ultimately apply not just to the physical surface figure of the optical component substrates, but to the wavefront produced by the complete imaging system. In addition to optical surface figure, the wavefront depends on the relative alignment of the individual optical components, and on significant aperture dependent phase shifts caused by the resonant multilayer reflective coatings. Recent analysis has shown that multilayer d-spacing nonuniformities that are small enough to ensure uniform illumination within desired tolerances, may nevertheless introduce significant wavefront phase errors.[2] Such phase errors cannot be detected by the visible-light interferometery which forms the current standard in surface figure measurement. For these and other reasons, at-wavelength interferometric testing will be a necessary metrology tool for the successful development of optics for EUV lithography.[3] Ultimately, the resolution enhancement offered by at-wavelength measurements may improve the accuracy of visible light interferometry through the creation of improved optical reference surfaces. Previous experiments involving knife-edge testing[4,5] have already demonstrated the benefits of testing at the functional wavelength for *in situ* alignment and characterization of EUV optics. Focalometry experiments and knife-edge tests have been performed on EUV optics.

The point diffraction interferometer[6,7] (PDI) has previously been proposed[8] as an attractive configuration for EUV at-wavelength testing: it utilizes a diffracted spherical reference wavefront, eliminating the need for optical reference surfaces or beamsplitters. The PDI provides a direct at-wavelength measurement of the wavefront from a single optical element or a compound optical system. It can also be used as an *in situ* alignment tool.

We have implemented and successfully operated a point diffraction interferometer using an undulator radiation source and coherent optics beamline at the Advanced Light Source (ALS) at Lawrence Berkeley Laboratory. Our first experiments have been characterization of elements of the interferometer, including the diffracted reference wavefront, and measurements of the EUV wavefront produced by a Fresnel zone plate lens. Intentional introduction of aberrations into the system are consistent with measured interference patterns.

0-8194-1785-8/95/$6.00

3. EXPERIMENT DESCRIPTION

The PDI, shown schematically in Fig. 1, consists of a partially transmitting membrane, containing a pinhole located near the focal plane of the optical element or optical system under test. The pinhole should be smaller than the diffraction limited focal spot. The central Airy disk of a spherical wavefront diffracted by the pinhole interferes with the transmitted wavefront from the optical system.

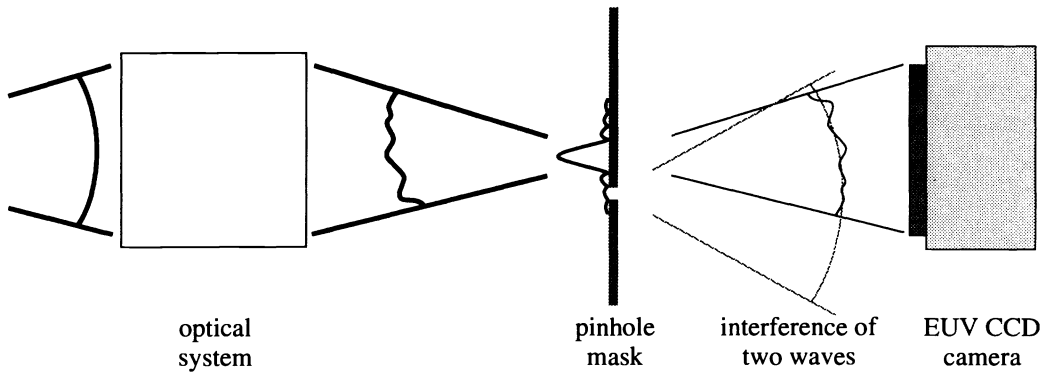

Figure 1. A schematic description showing the key elements of the PDI (not drawn to scale.) The optical system is illuminated using spatially coherent radiation. A small pinhole in a thin absorbing mask placed at the focus of an optical system generates a spherical reference wavefront. Interference fringes are recorded by an EUV CCD camera.

The PDI membrane used in these experiments was fabricated according to the prescription proposed by Sommargren and Hostetler,[8] and performed by Spallas, *et al.*[9] In this scheme a single PDI "mask" contains a square, 7×7 array of pinholes. Pinhole size varies in one direction, and absorber thickness varies in the perpendicular direction. In this way a pinhole which produces optimum numerical aperture, and fringe contrast may be selected. The pinholes, separated by 40 μm spacing, are adequately far apart to allow illumination of individual pinholes.

The mask consists of a 2000 Å thick Si_3N_4 membrane using a metallic Co film as the absorber. The pinholes were patterned by e-beam lithography, and were etched completely through the Si_3N_4 membrane before the Co film deposition. Using a carefully controlled thermal evaporation process, the graded Co film was deposited on the etched membrane in such a way as to maintain the open pinholes through the Co film as well. The Co film thickness varied across the mask from ~400 – 700 Å. The pinhole size required to produce a reference wavefront which overfills a 0.1 numerical aperture is on the order of 1600 Å. The effects of pinhole size are discussed in the following sections.

The pinhole mask is attached to a specially constructed *x-y* stage with 0.01 μm motion resolution and stability over a range of several millimeters. The interferometer is mounted on an optical table to provide the stability required for the experiment. The entire system operates at a vacuum of approximately 2×10^{-6} torr. Interferograms are recorded using an EUV CCD camera which incorporates a Tektronix 1024×1024 pixel, back-illuminated CCD, with 25×25 μm pixel size, and ~1 square inch total area.

The light source used in these experiments is a coherent optics undulator beamline operating at the Advanced Light Source (ALS) at Lawrence Berkeley Laboratory. The wavelength resolution of the spherical grating monochromator is $\lambda/\Delta\lambda \approx 3000$ (FWHM) at 13 nm wavelength, much greater than what is required for our experiments. The flux through the entrance to the interferometer is in the range of 10^6—10^8 photons per second, depending on experimental conditions. For our experiment, spatial coherence is determined by spatial filter entrance pinholes of 20 to 120 μm diameter. A future beamline design, optimized for the PDI, will increase the flux by up to three orders of magnitude.[10] This increase will be particularly significant for experiments involving reflective optical systems with large numerical aperture.

4. REFERENCE WAVEFRONT CHARACTERIZATION

The accuracy of the interferometer is limited by the quality of the spherical reference wavefront. The wavefront to be measured (the "test" wavefront) is compared to the diffracted reference wavefront, where the difference is measurable by interference fringes. In order to properly fill the numerical aperture of the optical system, it is essential that the pinhole be sufficiently small. The finite thickness of the absorbing substrate, and the shape of the diffracting pinhole may affect the quality of the reference wavefront.[11] Detailed numerical studies of these effects are in progress. Preliminary research suggests that for sufficiently small pinholes these deleterious effects will be small. We are interested in testing optical systems with a numerical aperture of approximately 0.1. The maximum pinhole diameter required to fill this numerical aperture at 13.5 nm wavelength is on the order of 1600 Å. Pinholes smaller than this upper limit may improve the quality of the reference wavefront, yet would require a greater attenuation of the test wavefront to achieve high contrast fringes, and an increased exposure time.

In order to measure the mask pinhole sizes, and to characterize the reference wavefront, a 50 μm circular aperture, placed within 5 mm of the mask, was used to illuminate individual mask pinholes. In this configuration, with no optical system in place, the diffraction pattern from each one of the entire 7 × 7 array of mask pinholes was measured at 12.4 nm wavelength.

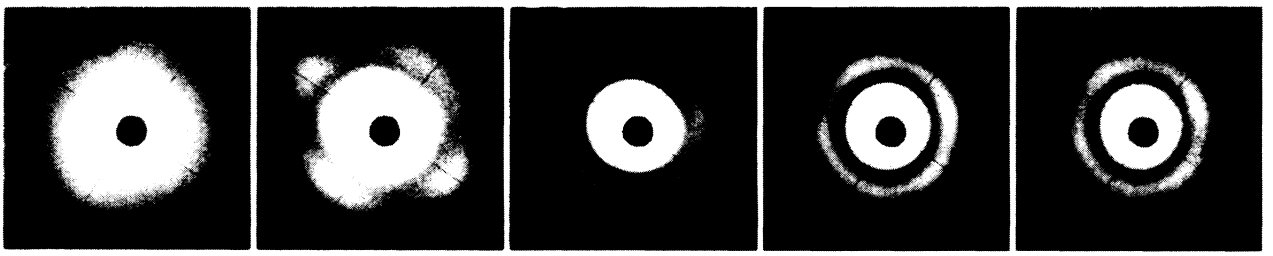

1400 Å 2400 Å 2800 Å 3100 Å 3200 Å

Figure 2. Five diffraction patterns from individually illuminated mask pinholes are shown here. Measured effective pinhole diameters appear below each image. These five pinholes belong to one mask row, with increasing pinhole size and constant absorber thickness. A small opaque disk is suspended in the center of the field of view to protect the CCD from damage due to saturation in other experiments.

Five diffraction patterns representing a row of pinholes with increasing diameter, and constant absorber thickness, are shown in Fig 2. These pinholes were located in the thickest part of the absorber substrate We determined the effective pinhole sizes from the diameters of the first minimum ring of the Airy-like diffraction patterns. The pinhole dimensions determined from the diffraction patterns here are consistent with the pinhole sizes observed by electron microscopy.

Technology for fabricating pinholes down to 100 nm diameter has been previously demonstrated.[12] We are currently pursuing several techniques to improve our pinhole masks, and hence the quality of the reference wavefront.

5. FRESNEL ZONE PLATE STUDY

We present here a description of the EUV wavefront produced by a Fresnel zone plate lens. Zone plates lenses are important elements in many short-wavelength applications which require concentrating or imaging elements. The study of zone plates is also an important first experiment for the development of future interferometer configurations which may utilize zone plates.

The zone plates studied here were fabricated in electroplated Ni, on a Si_3N_4 membrane. Each zone plate has a diameter of 200 μm, an outer zone width of 75 nm, and a focal length of 1.3 mm at 122 Å wavelength. Spatially coherent illumination of the zone plate is achieved by a 20–120 μm diameter entrance pinhole located 2.4 meters away. Under these conditions, the entrance pinhole "object" is unresolved by the zone plate lens, and in the absence of aberrations, a diffraction-limited focal spot will be produced by the zone plate with a central Airy disk diameter of ~1900 Å in the plane of the first-order focus. In

some experiments, the entrance pinhole was removed to substantially increase the illumination, but in this configuration, the spatial coherence cannot be guaranteed.

Fresnel zone plates diffract light into many separate diffraction orders, including undeviated zero-order light, higher focused orders, and divergent negative orders. To block light from these other orders, a 60 μm diameter opaque central stop in the zone plate is used in conjunction with a 50 μm diameter order-sorting aperture, placed at a distance of ~1 mm from the zone plate, as shown in Fig. 3. The central stop gives the zone plate an annular pupil.

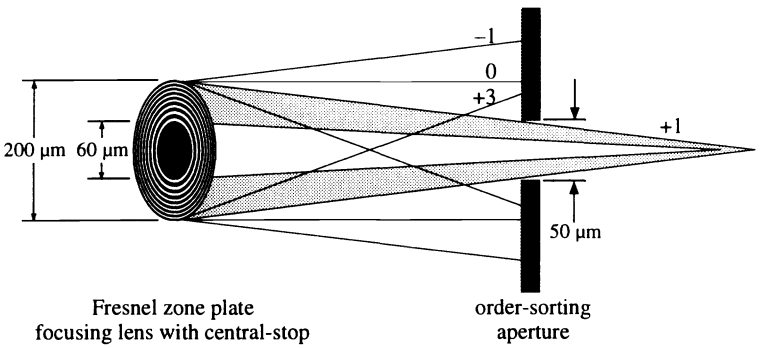

Figure 3. Schematic of zone plate diffraction showing four of the many diffracted orders. An order-sorting aperture is used in combination with an opaque central stop to block all but the first-order focused diffraction.

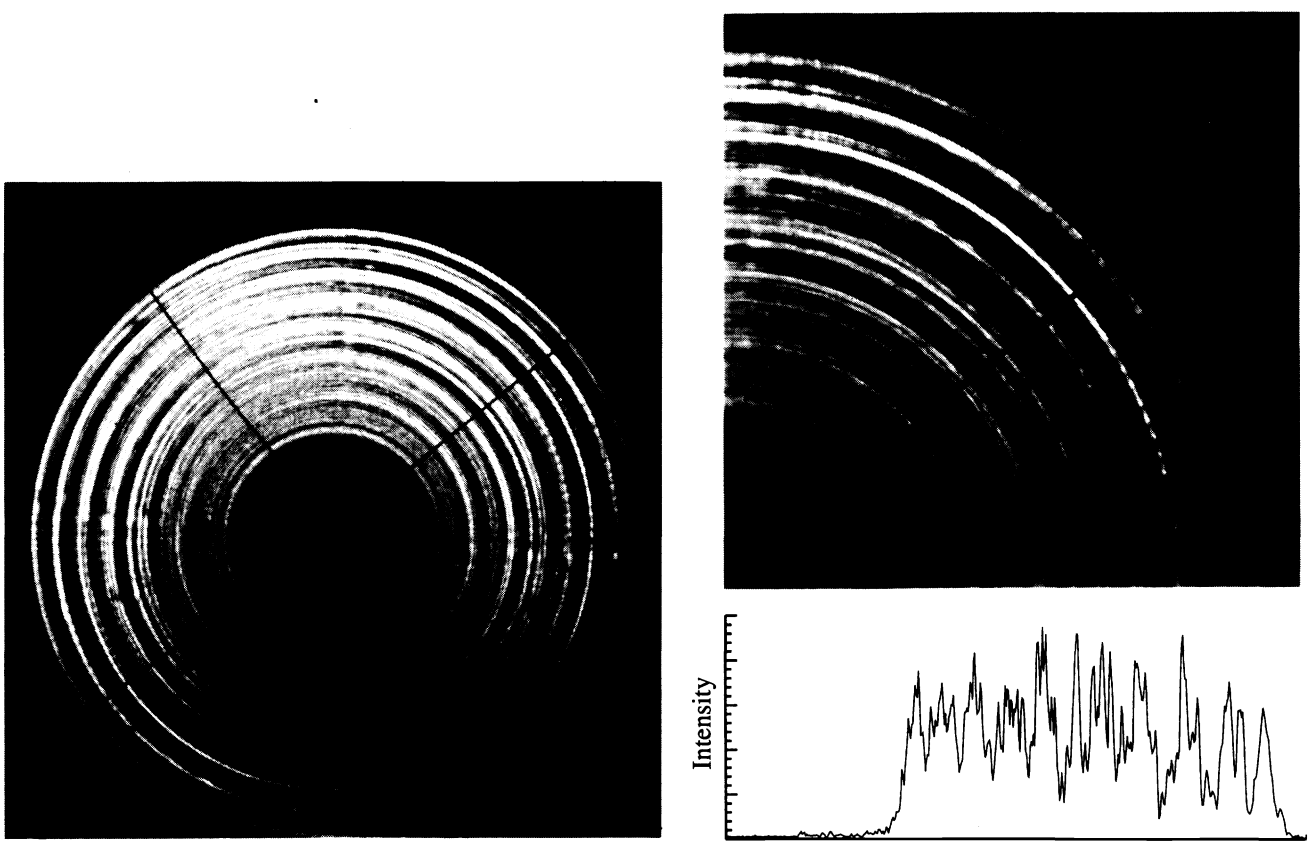

Figure 4. Positive-first-order diffracted light from a Fresnel zone plate lens, recorded 10 cm from the focus. On the right is a detail of the upper-right quadrant of the image, and an intensity cross-section taken from the bottom row of the detail. The cross section shows the characteristic magnitude and spatial frequency of the intensity modulation. These images are not interferograms; they are the unobstructed first-order diffracted light from a zone plate.

Measurements of the positive-first-order diffracted (focused) light from several similar zone plate lenses, recorded by an EUV CCD camera placed 10 cm from the zone plate, contain several consistent yet unanticipated results. These measurements, which reveal the intensity distribution of the zone plate wavefront, were recorded with the pinhole mask removed from the interferometer. In all thirteen of the zone plates we have measured, we observe very high spatial frequency "rings" of nearly 100 percent intensity modulation, throughout the entire annular region of illumination, (see Fig. 4.). Near the inner and outer edges of the annular illumination region, broader modulation, characteristic of edge-diffraction, is apparent. Diffracted light is visible in the regions within the center of the annulus and beyond the outer edge of the illuminated region.

The large, circular, light and dark rings are visible as unique patterns in each of the 13 zone plates we have measured. Some zone plates show less of this large scale modulation, and appear to be better than others in this regard. The presence of these rings is consistent with measured random zonal errors, and thermal drift introduced during the electron beam writing of the zone plate manufacture.[13] During the 20 minute electron beam exposure, drift is repeatedly compensated by re-registration to alignment marks.[14]

Preliminary interferometric measurements presented in the following section reveal that these rings, with their high spatial frequency modulation and non-uniform distribution, may be comparable to surface roughness in reflecting or refracting optical systems. Despite their presence, lower-ordered wavefront aberrations are still easily observed.

6. INTERFEROMETRIC RESULTS

At the highest resolution of the CCD camera, interferogram exposure times are typically 10 to 20 seconds. Lower resolution images, recorded with hardware binning of the CCD pixels, are typically exposed and displayed at a rate of one frame per second, allowing real-time alignment of the system. Interferograms successfully recorded with exposure times of several minutes suggest that the stability of the stages, the optical table, and the light source meet the necessary requirements of the sensitive measurements being performed.

6.1 Interferograms with high spatial frequency fringes

We are regularly able to record interferograms which display high spatial frequency and good fringe contrast. Two examples are shown in Fig. 5. In Fig. 5a, defocus is introduced by the displacement of the pinhole mask by several microns from the zone plate's focal plane in the longitudinal direction. Lateral displacement of the pinhole from the optic axis introduces wavefront "tilt" and causes the center of the defocus pattern to shift from the image center. In Fig. 5b the pinhole mask is very nearly in the focal plane of the zone plate. Lateral displacement here results in straight "tilt" fringes. To improve the fringe visibility, both images in Fig. 5 have undergone background subtraction, in which an image of the test wavefront, recorded through a clear section of the pinhole mask, is subtracted from the image recorded with the pinhole in place. These "difference" images reduce the appearance of the high spatial frequency modulation, and enhance the visibility of the fringes.

Figure 6 shows the results of fringe pattern analysis of the interferogram in Figure 5b. The lowest order aberrations representing displacements of the mask pinhole from the optic axis, and from the focal plane (tilt and defocus, respectively) have been removed. Using a fringe pattern analysis technique which follows the fringe minima to determine contours of constant phase, a phase map was generated over the annular illumination region.

As described in Section 4, if the central Airy disk of the reference wavefront does not overfill the numerical aperture of the optical system, significant intensity and phase variations across the recorded image may occur. Areas of low fringe visibility separating the regions of similar phase support the hypothesis that in this particular interferogram, the reference wavefront does not adequately fill the numerical aperture of the optical system.

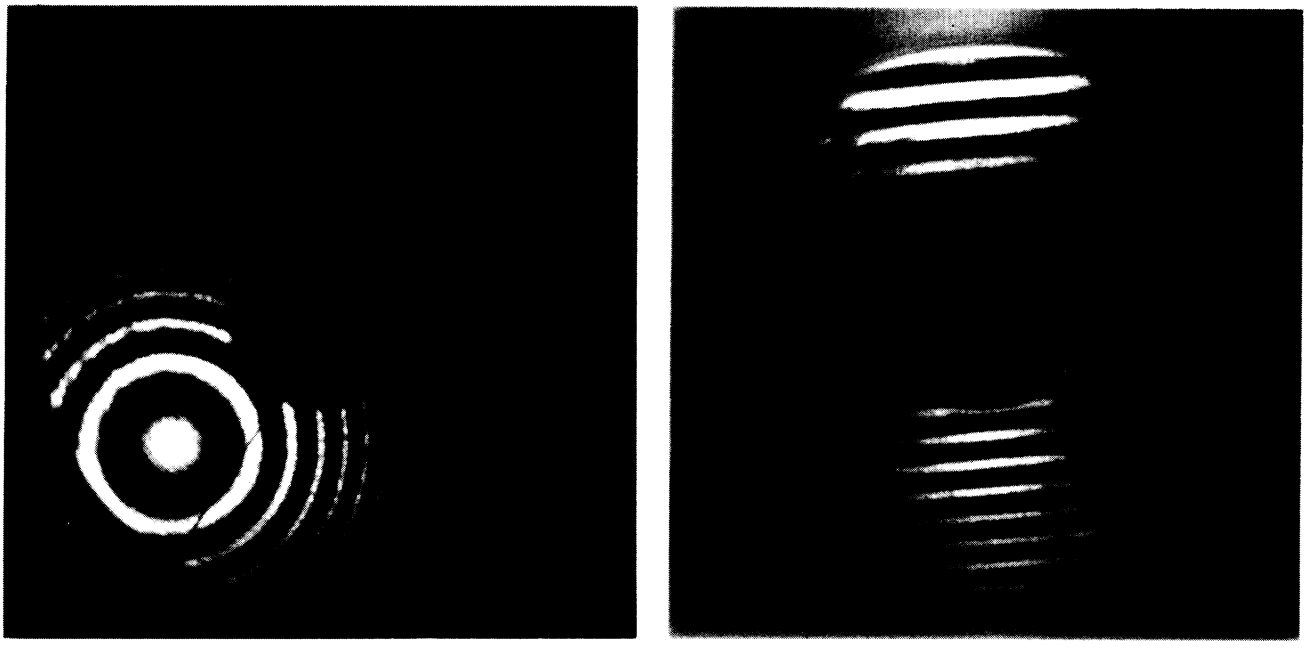

(a) (b)

Figure 5. Interferograms of a Fresnel zone plate showing fringe patterns characteristic of defocus (a), and tilt (b). The exposure times were 3 and 4 seconds respectively, and the wavelength was 122 Å.

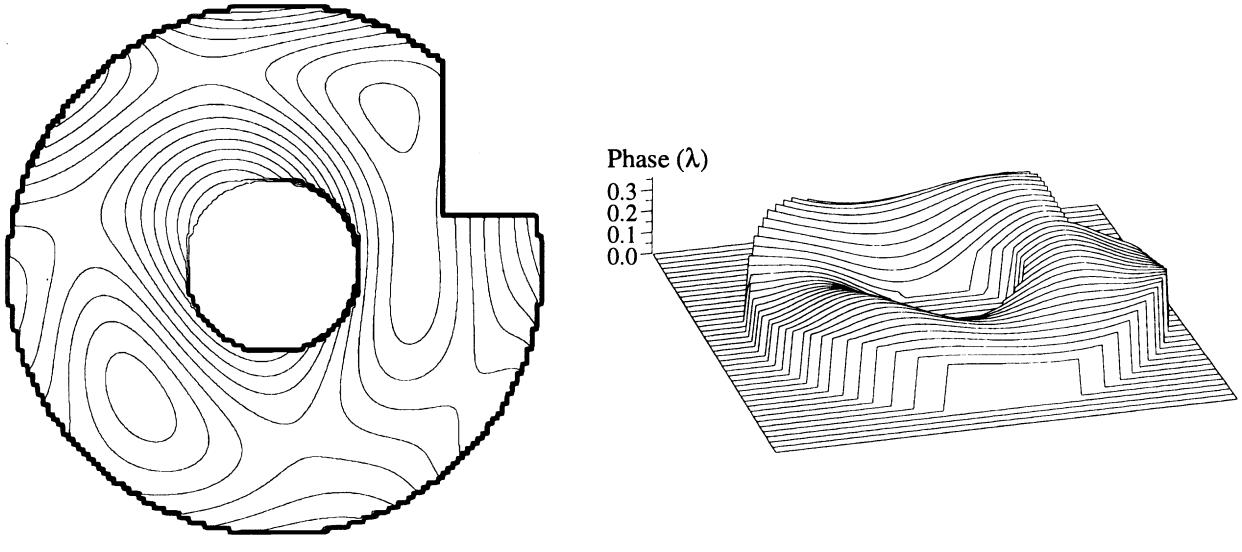

(a) (b)

Figure 6. Analysis of the interferogram shown in Fig. 5b. The zone plate's diffracted wavefront, measured at the CCD detector, is represented as a wavefront phase map. In (a) the contours are separated by 0.025 λ. The wavefront analysis shows a peak-to-valley measurement of 0.334 λ = 4.15 nm, and rms of 0.060 λ = 0.749 nm. However, in this interferogram, the quality of the reference wavefront cannot be guaranteed. A region of low fringe contrast and "forked" fringes was intentionally removed from the interferogram analysis.

6.2 Intentional introduction of astigmatism

An experiment was conducted to verify the qualitative behavior of the interferometer under the intentional introduction of aberrations. For this experiment, a slight x-direction tilt was introduced into the zone plate mount, forming an angle of approximately 5° between the optic axis and the zone plate normal. The primary aberration associated with this misalignment is astigmatism — the zone plate focal length along the tilted x-axis becomes slightly shorter than the unchanged focal length along the y-axis.

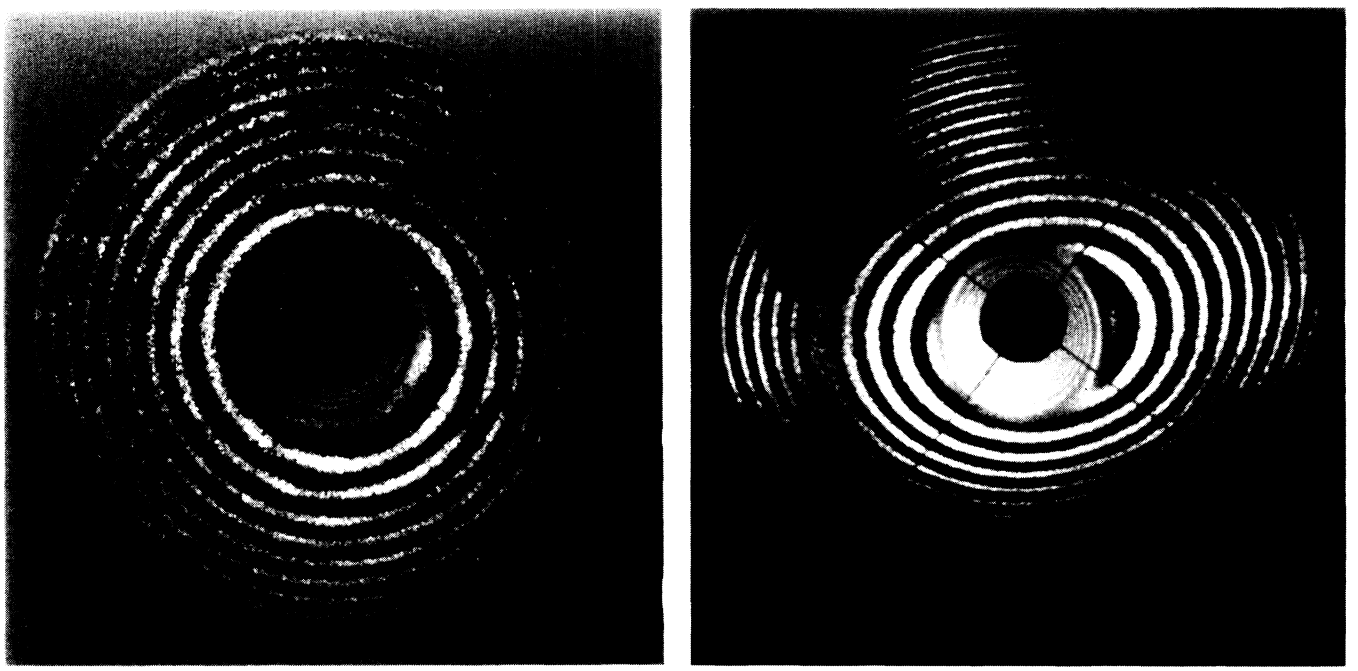

(a) Defocus (b) Astigmatism plus defocus

Figure 7. A comparison of two Fresnel zone plate interferograms recorded by the PDI. In (a) the zone plate is properly mounted; the pinhole mask is displaced from the focal plane causing the characteristic fringe patterns seen here. In (b) a the zone plate mount has been intentionally tilted by 5°.

Figure 7 displays a comparison of two interferograms. In Fig. 7a, the zone plate was properly mounted; while in 7b, the tilt described above was introduced. Displacement of the pinhole mask by several microns from the focal plane of the zone plate yields the circular fringe pattern characteristic of defocus. In Fig. 7b, the amount of focal error is different for the x- and the y-axes, creating an elliptical fringe pattern characteristic of astigmatism with defocus. Close inspection of the interferograms in Fig. 7 reveals regions of poor fringe contrast and fringe splitting. These characteristics may indicate either poor spatial coherence of the zone plate illumination (controlled by the size of the system's entrance pinhole) or a reference wavefront which does not fill the numerical aperture.

7. CONCLUSION

A prototypical point diffraction interferometer is operational at the Advanced Light Source, at Lawrence Berkeley Laboratory, and has been used to record interferometric fringe patterns of Fresnel zone plate lenses at EUV wavelengths. Preliminary experiments have been performed to characterize the interferometer. Other interferometric measurements have demonstrated the proper behavior of the zone plates with the intentional introduction of astigmatism. We are pursuing several techniques to improve our pinhole masks, and hence the quality of the reference wavefront.

After our initial experiments with Fresnel zone plate lenses, our future applications of the PDI will include measurement of reflective optical systems. We are collaborating with AT&T and Sandia National Laboratory to measure a 10x Schwarzschild objective, and with Lawrence Livermore National Laboratory to measure an EUV imaging system.

8. ACKNOWLEDGMENTS

This work was supported by the ARPA Advanced Lithography Program.

9. REFERENCES

1. M. D. Himel, in Soft X-Ray Projection Lithography, A. M. Hawryluk, and R. H. Stulen, eds. (Optical Society of America, Washington, DC 1993), 18, 1089.
2. J. Underwood, private communication.
3. D. Attwood, G. Sommargren, R. Beguiristain, K. Nguyen, J. Bokor, N. Ceglio, K. Jackson, M. Koike, J. Underwood, Appl. Opt. 32, 7022 (1993).
4. E. L. Raab, D. M. Tennant, W. K. Waskiewicz, A. A. MacDonald, *et. al,* J. Opt. Soc. Am. A 8, 1614 (1991)
5. A. K. Ray-Chaudhuri, R. H. Stulen, W. Ng, F. Cerrina, *et. al,* in Extreme Ultraviolet Lithography, D. T. Attwood and F. Zernike, eds. (Optical Society of America, Washington, D. C., 1994).
6. W. P. Linnik, Proceedings of the Academy of Sciences of the U.S.S.R. 1, 208 (1933)
7. R. N. Smartt, and W. H. Steel, Japan. J. of Appl. Phys. 14, (Suppl. 14-1), 351 (1975)
8. G. E. Sommargren, R. Hostetler, in Soft X-Ray Projection Lithography, A. M. Hawryluk, and R. H. Stulen, eds. (Optical Society of America, Washington, DC 1993), 18, 100-104.
9. J. P. Spallas, R. Hostetler, G. E. Sommargren, (to be published).
10. Preliminary calculations from a proposed beamline design. J. Underwood, private communication.
11. K. A. Goldberg, J. Bokor, R. Beguiristain, H. Medecki, *et. al,* in Extreme Ultraviolet Lithography, D. T. Attwood and F. Zernike, eds. (Optical Society of America, Washington, D. C., 1994).
12. D. M. Tennant, E. L. Raab, M. M. Becker, M. L. O'Malley, *et. al,* J. Vac. Sci. Technol. B 8, 6, 1970-74 (1990).
13. Erik H. Anderson, *et. al,* J. Vac. Sci. Technol. B 9, 6, 3606-11, (1991).
14. Erik H. Anderson. Private communication.